

# Relationship between the isotope effects on transition temperature, specific heat, and penetration depths

T. Schneider

*Physik-Institut der Universität Zürich, Winterthurerstrasse 190, CH-8057 Zürich, Switzerland*

(Received 31 October 2002; published 8 April 2003)

We show that in anisotropic superconductors, falling at finite temperature into the three-dimensional  $XY$  (3D- $XY$ ) and at zero temperature into the two-dimensional  $XY$  quantum superconductor to insulator transition (2D- $XY$ -QSI) universality class, the isotope effects on transition temperature, specific heat, and magnetic penetration depths are not independent, but related by universal relations. The corresponding experimental data for cuprate superconductors reveals suggestive consistency with these relations. They imply a dominant role of fluctuations so that pair formation and pair condensation do not occur simultaneously. For this reason and due to the occurrence of the 2D- $XY$ -QSI transition the isotope effects do not provide information on the underlying pairing mechanism but must be attributed to a shift of the phase diagram upon isotope substitution. The 2D-QSI transition is driven by the exchange of pairs, which favors superconductivity and the combined effects of disorder and Coulomb repulsion of the pairs, which favor localization. Since isotope substitution will hardly affect disorder and Coulomb repulsion, the shift of the phase diagram must be attributed to the electron-phonon interaction, which renormalizes the mass of the fermions and with that the mass and the exchange of the pairs.

DOI: 10.1103/PhysRevB.67.134514

PACS number(s): 74.20.Mn, 74.25.Dw

## I. INTRODUCTION

Isotope effect measurements were of crucial importance in establishing the phonon-induced BCS model of superconductivity<sup>1</sup>. In the weak-coupling BCS model the isotope effect derives from the superconducting transition temperature  $T_c$  being proportional to the Debye temperature. Since the Debye temperature is proportional to  $M^{1/2}$ , where  $M$  is the atomic mass, the isotope-effect coefficient for the transition temperature is  $\beta_{T_c} = -d \ln T_c / d \ln M = 0.5$ . The later inclusion of Coulomb repulsion in the pairing interaction resulted in predicted values of less than 0.5 and enabled a reasonably good fit to the data.<sup>2</sup> The situation is more complex in cuprate superconductors, where  $\beta_{T_c}$  is small near optimal doping and maximum  $T_c$  and large close to the quantum superconductor to insulator (QSI) transition where  $T_c$  vanishes.<sup>3-5</sup> Moreover, recently it has been shown that the effect of isotope substitution is not restricted to  $T_c$ , but affects the in-plane penetration depth as well.<sup>5-9</sup>

The main purpose of this paper is to demonstrate that this unconventional behavior of the isotope coefficients of  $T_c$ , in-plane penetration depth, etc., is caused by the dominant role of disorder, thermal and quantum fluctuations and not related to the pairing mechanism. This differs fundamentally from conventional superconductors, where fluctuations do not play an essential role so that the formation of pairs and their condensation occur essentially simultaneously and where the isotope effect allowed us to identify the electron-phonon interaction as the dominant pairing interaction. Our starting point is the phase transition surface  $T_c(x, y, M)$  where  $x$  is related to the hole concentration,  $y$  denotes the substituent concentration, e.g., for Cu, or the strength of disorder and  $M$  is the isotope mass. Cuprates where these parameters can be varied include  $\text{La}_{2-x}\text{Sr}_x\text{Cu}_{1-y}\text{A}_y\text{O}_4$  ( $A = \text{Ni}, \text{Zn}, \dots$ ) and  $\text{Y}_{1-x}\text{Pr}_x\text{Ba}_2\text{Cu}_3\text{O}_{7-\delta}$ , using for Cu pure  $^{63}\text{Cu}$  or  $^{65}\text{Cu}$ , or for O pure  $^{16}\text{O}$  or  $^{18}\text{O}$ . In Fig. 1 we dis-

played the phase-transition surface  $T_c(x, y)$  for  $\text{La}_{2-x}\text{Sr}_x\text{Cu}_{1-y}\text{Zn}_y\text{O}_4$ .  $T_c$  vanishes for  $y=0$  in the so-called underdoped limit  $x=x_u$ , increases for  $x>x_u$  and reaches its maximum value at optimum doping  $x=x_m$ . For any doping level where superconductivity occurs  $x_u \leq x \leq x_m$  the transition temperature is reduced upon Zn substitution and vanishes along the line  $y_c(x)$  of quantum phase transitions. The doping dependence of the anisotropy and the temperature dependence of the resistivity indicate that along this line two-dimensional quantum superconductor to insulator (2D-QSI) transitions occur for  $x \approx 0.19$ , while for  $x \approx 0.19$  three-dimensional quantum superconductor to normal state (3D-QSN) transitions take place.<sup>10-13</sup> Here we concentrate on the underdoped regime,  $x_u \leq x \leq x_m$ . Since the anisotropy, defined as the ratio  $\gamma = \xi_{ab} / \xi_c$  of the correlation lengths parallel ( $\xi_{ab}$ ) and perpendicular ( $\xi_c$ ) to  $\text{CuO}_2$  layers ( $ab$  planes) and evaluated at  $T_c$ , tends to diverge by approaching the endline  $y_c(x)$ , a three- to two-dimensional (3D-2D) cross-over occurs.<sup>13-15</sup> Moreover, the order parameter is a complex scalar, corresponding to a two component vector ( $XY$ ). Accordingly, for  $x_u \leq x \approx 0.19$ ,  $y_c(x)$  is a line of 2D- $XY$ -QSI transitions. On the other hand, there is mounting evidence that at finite temperature the critical properties associated with the phase-transition surface  $T_c(x, y, M)$  appear to fall into the 3D- $XY$  universality class.<sup>13-15</sup> Supposing that the 2D- $XY$ -QSI and 3D- $XY$  universality classes hold true, this leads naturally to universal critical amplitude combinations, involving the transition temperature and the critical amplitudes of specific heat and penetration depths, which also apply to the isotope effects. They yield universal relations between the isotope coefficients for the transition temperature, the penetration depths, and the specific heat.

In Sec. II we sketch the universal relations for anisotropic superconductors falling at finite temperature into the 3D- $XY$  and at zero temperature into the 2D-QSI universality class. Since fluctuations are supposed to dominate, pair formation

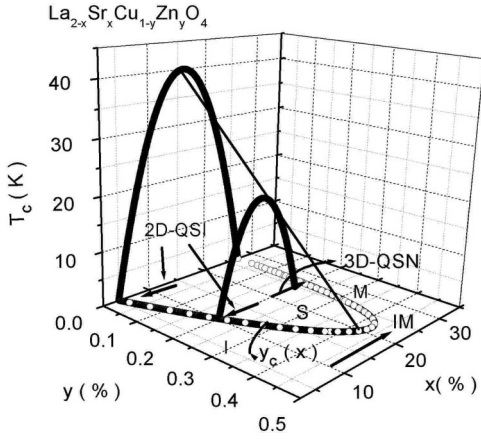


FIG. 1.  $T_c(x,y)$  phase diagram of  $\text{La}_{2-x}\text{Sr}_x\text{Cu}_{1-y}\text{Zn}_y\text{O}_4$  derived from the resistivity data of Momono *et al.* (Ref. 10) and Fukuzumi *et al.* (Ref. 11).  $y_c(x)$  is a line of quantum phase transitions. The arrows mark two-dimensional quantum superconductor to insulator (2D-QSI,  $x \sim 0.19$ ), three-dimensional quantum superconductor to normal state transition (3D-QSN,  $x \sim 0.19$ ), and insulator to normal state (IM) crossover, respectively.

and pair condensation do not occur simultaneously. For this reason, the universal relations between transition temperature and the critical amplitudes of specific heat, correlation lengths, and penetration depths do not depend on the underlying pairing mechanism, but reveal how the isotope effects on these quantities are correlated. To explore the nature of the isotope effects we concentrate on the regime where the materials flow to 2D-QSI criticality, driven by variation of dopant concentration  $x$  and  $y$ , e.g., the concentration of substituents for Cu or the strength of disorder. In this regime, the essential effect of isotope substitution is a slight depression of the phase-transition surface  $T_c(x,y)$  which unalterably implies a shift of the quantum phase-transition line  $y_c(x)$  and of the underdoped limit  $x_u$ .<sup>5,15</sup> Using this facts and the scaling theory of quantum critical phenomena it is shown that the flow to 2D-QSI criticality is characterized by an anomalous increase of the isotope coefficient for the transition temperature  $\beta_{T_c}$ , zero-temperature in-plane penetration depth  $\beta_{1/\lambda_{ab}^2(0)}$  and condensation energy  $\beta_E$ , given by  $\beta_{T_c} \propto \beta_{1/\lambda_{ab}^2(0)} \propto \beta_E \propto T_{cm}/T_c$ , irrespective along which axis the 2D-QSI critical point is approached.  $T_{cm}$  denotes the maximum transition temperature within a family of cuprates.

A comparison with experiment is presented in Sec. III. Although the data on the isotope effect on transition temperature and the critical amplitudes of the penetration depths are rather sparse, they reveal suggestive consistency with this scenario. We hope that the present paper will serve as a stimulus for future systematic measurements. On the contrary, the experimental data on the  $T_c$  dependence of  $\beta_{T_c}$  allows a rather quantitative comparison with our predictions. Irrespective of the path along which the 2D-QSI critical point is approached, our prediction,  $\beta_{T_c} \propto T_{cm}/T_c$  is well confirmed, including the spin-triplet  $p$ -wave superconductor  $\text{Sr}_2\text{RuO}_4$ . Here, reduced  $T_c$ 's were achieved by using crystals containing impurities and defects.<sup>16</sup> Intriguingly enough

the factor of proportionality appears to adopt a nearly unique value, indicating that  $\beta_{T_c} \approx 0.17 T_{cm}/T_c$  holds, independent of the material and the direction of the flow to 2D-QSI criticality. A potential candidate for the description of the 2D-QSI transition are 2D disordered bosons with long-range Coulomb interactions.<sup>5,14,15,17-19</sup> Here the transition is driven by the competition between exchange of pairs, which favors superfluidity, and the combined effects of disorder and the Coulomb interaction, which favor localization.

## II. UNIVERSAL RELATIONS

The universality class to which the cuprates at finite temperature belong is not only characterized by its critical exponents but also by various critical-point amplitude combinations which are equally important. Though these amplitudes depend on  $x, y$ , and  $M$ , their universal combinations do not. An important example is the universal relation<sup>14,15,20</sup>

$$(k_B T_c)^3 = \left( \frac{\Phi_0^2}{16\pi^3} \right)^3 \frac{\xi_{x0}^{tr} \xi_{y0}^{tr} \xi_{z0}^{tr}}{\lambda_{x0}^2 \lambda_{y0}^2 \lambda_{z0}^2}, \quad (1)$$

where  $\xi_{i0}^{tr}$  and  $\lambda_{i0}$  are the critical amplitude of the transverse correlation lengths and the penetration depths, respectively. These length scales diverge as

$$\xi_{i0}^{tr} = \xi_{i0}^{tr} |t|^{-\nu}, \quad \lambda_i = \lambda_{i0} |t|^{-\nu/2}. \quad (2)$$

Close to criticality the specific-heat singularity is characterized by

$$\frac{C}{Vk_B} = - \frac{T}{k_B} \frac{\partial^2 f_s}{\partial t^2} \approx \frac{A^\pm}{\alpha} |t|^{-\alpha}, \quad (3)$$

and the combination of the critical amplitude  $A^-$  and the transverse correlation volume,

$$(R^\pm)^3 = A^- \xi_{x0}^{tr} \xi_{y0}^{tr} \xi_{z0}^{tr} = -Q_3^\pm \alpha (1-\alpha)(2-\alpha), \quad (4)$$

turns out to be universal as well.<sup>14,15,20</sup>  $R^\pm$  are universal numbers. Combining then the universal relations (1) and (4) we obtain a relation between measurable properties which holds at any finite temperature irrespective of the doping and substitution level:

$$T_c^3 = \left( \frac{\Phi_0^2}{16\pi^3 k_B} \right)^3 \frac{(R^-)^3}{A^- \lambda_{x0}^2 \lambda_{y0}^2 \lambda_{z0}^2}. \quad (5)$$

Considering variations in the dopant, substituent concentration, etc., denoted by  $y$  it then follows that the changes in  $T_c$ ,  $A^-$ , and  $1/\lambda_{i0}^2$  are not independent but related by

$$\frac{1}{T_c} \frac{dT_c}{dy} = - \frac{1}{3A^-} \frac{dA^-}{dy} + \frac{1}{3} \sum_{i=1}^3 \lambda_{i0}^2 \frac{d(1/\lambda_{i0}^2)}{dy}. \quad (6)$$

In tetragonal cuprates, where  $\lambda_{ab0} = \lambda_{a0} = \lambda_{b0}$ , it reduces to

$$\frac{1}{T_c} \frac{dT_c}{dy} = -\frac{1}{3A^-} \frac{dA^-}{dy} + \frac{2}{3} \lambda_{ab,0}^2 \frac{d(1/\lambda_{ab,0}^2)}{dy} + \frac{1}{3} \lambda_{c,0}^2 \frac{d(1/\lambda_{c,0}^2)}{dy}. \quad (7)$$

In the underdoped regime, tuned by variation of the dopant, substitution, or impurity concentration, the cuprates undergo a 2D-QSI transition. Here the universal relation<sup>14,15</sup>

$$T_c = \frac{\Phi_0^2 \bar{R}_2 d_s}{16\pi^3 k_B} \frac{1}{\lambda_{ab}^2(0)} \quad (8)$$

between transition temperature and zero-temperature in-plane penetration depth holds.  $d_s$  denotes the thickness of the superconducting sheets and  $\bar{R}_2$  is a universal dimensionless constant. Considering variations in the dopant, substituent concentration, etc., denoted by  $y$ , it then follows that the changes in  $T_c$ ,  $d_s$ , and  $1/\lambda_{ab}^2(0)$  are not independent but related by

$$\frac{1}{T_c} \frac{dT_c}{dy} = \frac{1}{d_s} \frac{dd_s}{dy} + \lambda_{ab}^2(0) \frac{d}{dy} \left( \frac{1}{\lambda_{ab}^2(0)} \right). \quad (9)$$

Thus the approach to 2D-QSI criticality is associated with a flow to

$$\begin{aligned} \frac{1}{T_c} \frac{dT_c}{dy} &\rightarrow \frac{1}{d_s} \frac{dd_s}{dy} + \lambda_{ab0}^2 \frac{d}{dy} \left( \frac{1}{\lambda_{ab0}^2} \right) \\ &\rightarrow \frac{1}{d_s} \frac{dd_s}{dy} + \lambda_{ab}^2(0) \frac{d}{dy} \left( \frac{1}{\lambda_{ab}^2(0)} \right), \end{aligned} \quad (10)$$

As the isotope substitution is concerned it is useful to rewrite Eq. (7) in the form

$$\beta_{T_c} = \frac{2}{3} \beta_{1/\lambda_{ab,0}^2} + \frac{1}{3} \beta_{1/\lambda_{c,0}^2} - \frac{1}{3} \beta_{A^-}, \quad (11)$$

where  $\beta_B$  is the isotope coefficient defined by

$$\beta_B = -\frac{M}{B} \frac{dB}{dM}. \quad (12)$$

$B = (T_c, \lambda_{ab,0}^2, \lambda_{c,0}^2, A^-)$  and  $dM = {}^{16}M - {}^{18}M$ . It reveals that a change of the transition temperature upon isotope substitution is unalterably linked to a change in the specific heat and the penetration depths. Note that a vanishing isotope effect on  $T_c$  merely implies that the contributions of specific heat and penetration depths cancel. In this context it is important to recognize that the universal relations, including Eqs. (5), (6), and (11) also apply in the presence of disorder. Indeed, since the critical exponent  $\alpha$  of the specific heat is negative in the 3D-XY universality class, Harris criterion implies that disorder is irrelevant at finite temperature.<sup>21</sup> On the other hand, close to 2D-QSI criticality the isotope coefficients of  $T_c$  and zero-temperature in-plane penetration depth are according to Eq. (9) related by

$$\beta_{T_c} = \beta_{d_s} + \beta_{1/\lambda_{ab}^2(0)}. \quad (13)$$

In analogy to Eq. (10), the approach to 2D-QSI criticality is then associated with the flow

$$\beta_{T_c} = \frac{2}{3} \beta_{1/\lambda_{ab,0}^2} + \frac{1}{3} \beta_{1/\lambda_{c,0}^2} - \frac{1}{3} \beta_{A^-} \rightarrow \beta_{d_s} + \beta_{1/\lambda_{ab}^2(0)}. \quad (14)$$

The 2D-QSI transition is also characterized by the scaling relations<sup>14,15</sup>

$$T_c = a_\delta \delta^{z\bar{\nu}}, \quad \bar{\xi}_{ab} = \bar{\xi}_{ab,\delta} \delta^{-\bar{\nu}}. \quad (15)$$

$\bar{\xi}_{ab}$  is the in-plane correlation length extrapolated to zero temperature and  $\delta$  measures the distance from the critical point with dynamic critical exponent  $z$  and correlation length exponent  $\bar{\nu}$ . In cuprates there is consistent evidence for a 2D-QSI transition with  $z=1$  and  $\bar{\nu} \approx 1$ .<sup>14,15</sup> These estimates coincide with the theoretical prediction for a 2D disordered Bosonic system with long-range Coulomb interactions.<sup>17-19</sup> This strongly suggests that in cuprate superconductors the loss of phase coherence, due to the localization of Cooper pairs, is responsible for the 2D-QSI transition.

To explore the scaling behavior of the isotope coefficient for the transition temperature  $\beta_{T_c}$  along the hole concentration axis  $x$  we can use the empirical relation

$$T_c(x) = \frac{2T_{cm}}{x_m^2} (x - x_u)(x_o - x), \quad x_m = \frac{x_u + x_o}{2}, \quad (16)$$

due to Presland *et al.*<sup>22</sup> It describes the phase-transition line of cuprate superconductors in the temperature-dopant concentration ( $x$ ) plane very well.<sup>23</sup> The hole concentration  $p$  can be varied effectively by changing the oxygen content and substitution in noncopper sites.  $T_c$  adopts its maximum value  $T_{cm}$  at optimum doping  $x = x_m$ .  $x_u$  denotes the underdoped and  $x_o$  the overdoped limit. Note that this empirical relation is fully consistent with a 2D-QSI transition with  $z\bar{\nu} = 1$  and  $\delta = (x - x_u)/x_u$ , because  $T_c(x) = [4T_{cm}/(x_o - x_u)](x - x_u) \approx T_{cm}(x - x_u)$ . The main effect of isotope substitution is the shift of  $x_u$  to a slightly larger value and of  $T_{cm}$  to a slightly lower value. Concentrating on the behavior close to 2D-QSI criticality, we obtain with Eq. (12) the expression

$$\beta_{T_c} = \frac{4x_u T_{cm}}{(x_o - x_u) T_c} \beta_{x_u} \approx \frac{T_{cm}}{T_c} \beta_{x_u}, \quad \beta_{x_u} = \frac{M}{x_u} \frac{dx_u}{dM}. \quad (17)$$

Thus the flow to 2D-QSI criticality along the hole concentration axis is characterized by the depression of  $T_c$ , giving rise to a divergent isotope coefficient  $\beta_{T_c}$ . The amplitude of the divergence is controlled by  $\beta_{p_u}$ , the isotope coefficient associated with the shift of the underdoped limit upon isotope substitution. Approaching the 2D-QSI critical point along the disorder or substitution (e.g., substitution for Cu) axis, denoted by  $y$ ,  $T_c$  vanishes as<sup>14,15</sup>

$$T_c = T_{cm} (1 - y/y_c)^{z\bar{\nu}}. \quad (18)$$

TABLE I. Estimates for  $\Delta T_c/T_c$  and  $\lambda_{ab0}^2 \Delta(1/\lambda_{ab0}^2)$  derived from the magnetic torque measurements of Hofer *et al.*<sup>8</sup> on  $\text{La}_{2-x}\text{Sr}_x\text{CuO}_4$  and the  $\mu\text{SR}$  measurements of Khasanov *et al.*<sup>9</sup> on  $\text{Y}_{1-x}\text{Pr}_x\text{Ba}_2\text{Cu}_3\text{O}_{7-\delta}$ .

	$x$	$T_c$ ( $^{16}\text{O}$ ) (K)	$\Delta T_c/T_c$	$\lambda_{ab0}^2 \Delta(1/\lambda_{ab0}^2)$
$\text{La}_{2-x}\text{Sr}_x\text{CuO}_4$	0.15	37.2	-0.008	-0.033
	0.086	22.19	-0.051	-0.062
	0.08	19.1	-0.073	-0.086
$\text{Y}_{1-x}\text{Pr}_x\text{Ba}_2\text{Cu}_3\text{O}_{7-\delta}$	0	91.4	-0.0044	-0.025
	0.3	57.2	-0.049	-0.072
	0.4	42.6	-0.059	-0.079

Upon isotope substitution  $y_c$  shifts to a slightly smaller value, because  $T_c$  is lowered (see Fig. 1). Concentrating then on the divergent part of  $\beta_{T_c}$  so that the effect on  $T_{cm}$  can be neglected we obtain with Eq. (12) and for  $z\bar{\nu}=1$  the expression

$$\beta_{T_c} = \frac{T_{cm}}{T_c} \beta_{y_c}, \quad \beta_{y_c} = -\frac{M}{y_c} \frac{dy_c}{dM}. \quad (19)$$

On the other hand, approaching the 2D-QSI critical point along the residual resistivity axis, there is the scaling relation<sup>14,15</sup>

$$T_c = T_{cm} (1 - \rho_{ab}/\rho_{ab}^c)^{z\bar{\nu}}, \quad (20)$$

where  $\rho_{ab}$  and  $\rho_{ab}^c$  denote the residual and critical residual in-plane resistivity, respectively. In the 2D limit the relevant measure of resistivity is the sheet resistance  $\rho^\square = d_s \rho_{ab}$ , adopting at criticality a fixed value,  $\rho^\square \approx h/(4e^2)$ .<sup>14,15,17,18</sup>

Considering  $z\bar{\nu}=1$  and approaching 2D-QSI criticality along the in-plane resistivity axis, the isotope coefficient  $\beta_{T_c}$  adopts then with Eq. (12) the form

$$\beta_{T_c} = \frac{T_{cm}}{T_c} \frac{M}{\rho_{ab}^c} \frac{d\rho_{ab}^c}{dM} = \frac{T_{cm}}{T_c} \beta_{d_s}, \quad \beta_{d_s} = -\frac{M}{d_s} \frac{dd_s}{dM}. \quad (21)$$

$\beta_{d_s}$  denotes the isotope coefficient of  $d_s$ , the thickness of the 2D slab. Since  $d_s$  remains finite upon isotope substitution, this also applies to  $\beta_{d_s}$ . Thus close to 2D-QSI criticality we obtain with Eqs. (13), (17), (19), and (21) the relation

$$\beta_{T_c} = \frac{T_{cm}}{T_c} \beta_{d_s} = \frac{T_{cm}}{T_c} \beta_{y_c} \approx \frac{T_{cm}}{T_c} \beta_{x_u} \approx \beta_{1/\lambda_{ab}^2(0)}, \quad (22)$$

revealing that  $\beta_{T_c} \propto T_{cm}/T_c$  holds with a unique factor of proportionality, irrespective of the axis the 2D-QSI critical point is approached.

Another quantity of interest is the condensation energy per unit volume. Close to 2D-QSI and 3D-QSN criticality its singular part scales as the inverse of the zero-temperature correlation volume, so that

$$-E(T=0) \propto \delta^{\bar{\nu}(D+z)} \propto T_c^{D+z}, \quad (23)$$

using Eq. (15). Thus along the quantum critical endline  $y_c(x)$  (see Fig. 1), the condensation energy vanishes, as it

should be. Invoking Eqs. (12) and (23) the isotope coefficient of the condensation energy adopts then close to the 2D-QSI critical point the form

$$\beta_E = -\frac{M}{E} \frac{dE}{dM} = (2+z) \beta_{T_c} \propto \frac{T_{cm}}{T_c}. \quad (24)$$

### III. COMPARISON WITH EXPERIMENT

We are now prepared to confront these predictions for the isotope effect with experiment. Although the experimental data on the isotope effect on transition temperature and penetration depth are rather sparse, some insight can be obtained from the estimates listed in Table I.  $\text{La}_{2-x}\text{Sr}_x\text{CuO}_4$  and  $\text{Y}_{1-x}\text{Pr}_x\text{Ba}_2\text{Cu}_3\text{O}_{7-\delta}$  undergo a doping tuned 2D-QSI transition at  $x \approx 0.05$  and  $x \approx 0.55$ ,<sup>24</sup> respectively.<sup>14,15</sup> These estimates have been derived from a fit of the experimental data for  $1/\lambda_{ab}^2(T)$ ,<sup>8,9</sup> to the leading critical behavior

$$\frac{1}{\lambda_{ab}^2} = \frac{1}{\lambda_{ab,0}^2} t^{2\nu}, \quad t = 1 - T/T_c, \quad \nu = 2/3. \quad (25)$$

An example is shown in Fig. 2. Since there is mounting evidence for 3D-XY criticality and the available data are rather sparse close to  $T_c$ , we kept  $\nu$  fixed. For this reason and in view of the excellent fits to both the  $\text{La}_{2-x}\text{Sr}_x\text{CuO}_4$  and  $\text{Y}_{1-x}\text{Pr}_x\text{Ba}_2\text{Cu}_3\text{O}_{7-\delta}$  data, the estimates quoted in Table

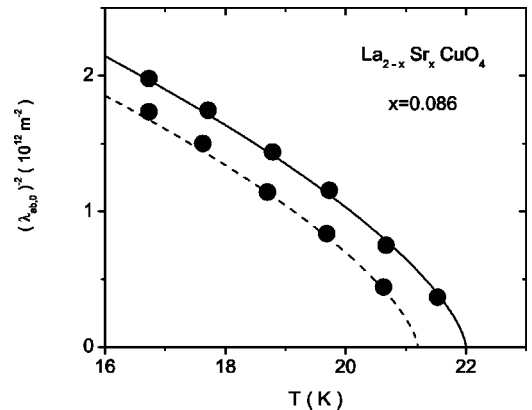


FIG. 2. Isotope effect on transition temperature and in-plane penetration depth in  $\text{La}_{2-x}\text{Sr}_x\text{CuO}_4$  at  $x=0.086$ . The upper ( $^{16}\text{O}$ ) and lower curve ( $^{18}\text{O}$ ) are fits to Eq. (25) yielding the parameters listed in Table I. Experimental data taken from Hofer *et al.* (Ref. 8).

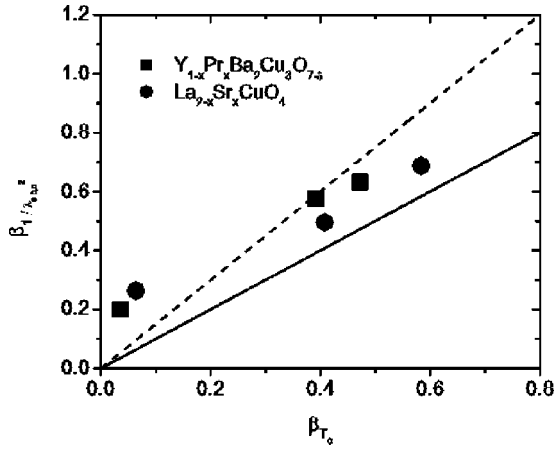


FIG. 3.  $\beta_{1/\lambda_{ab,0}^2}$  versus  $\beta_{T_c}$  for  $Y_{1-x}Pr_xBa_2Cu_3O_{7-\delta}$  (■:  $x=0, 0.3$ , and  $0.4$ ) and  $La_{2-x}Sr_xCuO_4$  (●:  $x=0.08, 0.086$ , and  $0.15$ ). The straight line is  $\beta_{1/\lambda_{ab,0}^2} = \beta_{T_c}$  and the dashed one is  $\beta_{1/\lambda_{ab,0}^2} = 3\beta_{T_c}/2$ . Data points taken from Table I.

I should be reliable and with that reveal the flow to 2D-QSI criticality. To uncover this flow we displayed in Fig. 3 the plot  $\beta_{1/\lambda_{ab,0}^2}$  versus  $\beta_{T_c}$ . Although the set of data points is sparse, key trends emerge. As  $T_c$  decreases the data points flow to the straight line, signaling the approach to 2D-QSI criticality, where  $\beta_{1/\lambda_{ab,0}^2} \rightarrow \beta_{1/\lambda_{ab,0}^2(0)} \rightarrow \beta_{T_c} \rightarrow \infty$  [see Eqs. (14) and (22)]. In this flow both cuprates appear to cross the dashed line, corresponding to  $\beta_{1/\lambda_{ab,0}^2} = 3\beta_{T_c}/2$ . Here the contributions of specific heat and out-of-plane penetration depth cancel [see Eq. (11)]. This clearly reveals that except for this special point the isotope effect on transition temperature and the critical amplitude of the in-plane penetration depth are not simply related. Indeed, the contributions of the specific heat and out-of-plane penetration depth cancel at this special point only. There is also the experimental fact that close to the maximum  $T_c$  the isotope effect on  $1/\lambda_{ab,0}^2$  is substantial, while it is very small in  $T_c$ . A glance to the universal relation (11) shows that even for  $\beta_{T_c} = 0$  a substantial isotope effect on the in-plane penetration depth can be expected, whenever the contributions of the specific heat and out-of-plane penetration depth do not cancel. Indeed, the absence of an isotope effect in one of the quantities entering Eq. (11) is not bound to the absence of an effect in all the others.

Additional evidence for the flow to 2D-QSI criticality stems from the plot  $1/\beta_{1/\lambda_{ab,0}^2(0)}$  versus  $1/\beta_{T_c}$  shown in Fig. 4 for the oxygen isotope effect in  $La_{2-x}Sr_xCuO_4$  (Refs. 8 and 7) and  $Y_{1-x}Pr_xBa_2Cu_3O_7$ .<sup>9</sup> It clearly reveals the crossover to the asymptotic 2D-QSI behavior, indicated by the dashed straight line, where  $\beta_{T_c} \rightarrow \beta_{1/\lambda_{ab,0}^2(0)}$ , because  $\beta_{d_s}$  remains finite, while  $\beta_{T_c} = T_{cm}\beta_{d_s}/T_c$  diverges [Eq. (22)]. For comparison we included the solid curve, which is Eq. (13), providing for  $\beta_{d_s}$ , the oxygen isotope coefficient of  $d_s$ , the estimate

$$\beta_{d_s} = -\frac{M}{d_s} \frac{dd_s}{dM} = -0.24. \quad (26)$$

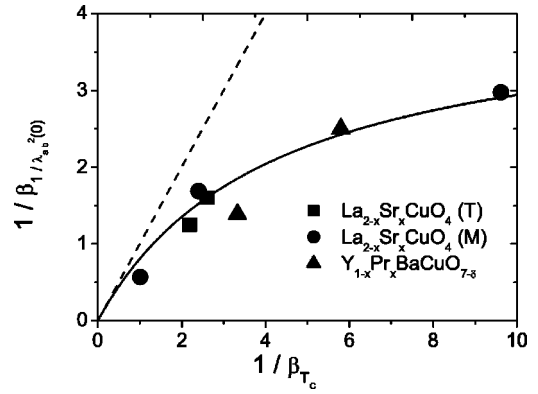


FIG. 4. Oxygen isotope effect in  $La_{2-x}Sr_xCuO_4$  and  $Y_{1-x}Pr_xBa_2Cu_3O_7$  in terms of  $1/\beta_{1/\lambda_{ab,0}^2(0)}$  versus  $1/\beta_{T_c}$ . The dashed line marks the critical behavior close to 2D-QSI criticality, that is Eq. (13) with  $\beta_{d_s} = 0$ , while the solid curve is Eq. (13) with  $\beta_{d_s} = -0.24$ , indicating the crossover due to the isotope effect on  $d_s$ .

This yields with Eq. (22)

$$\beta_{T_c} \approx 0.24 \frac{T_{cm}}{T_c}, \quad (27)$$

irrespective of the path the 2D-QSI transition is approached.

To clarify the uniqueness of this estimate for the factor of proportionality further, we follow our previous work.<sup>5</sup> In Fig. 5 we displayed the experimental data for  $YBa_{2-y}La_yCu_3O_7$ ,<sup>25</sup>  $La_{1.95}Sr_{0.15}Cu_{1-y}Ni_yO_4$ ,<sup>26</sup>  $Y_{1-x}Pr_xBa_2Cu_3O_7$  (Ref. 27) and  $Sr_2RuO_4$ <sup>16</sup> in terms of  $\beta_{T_c}$  versus  $T_c/T_{cm}$ . Note that  $Sr_2RuO_4$  is a spin-triplet  $p$ -wave superconductor with an intrinsic  $T_{c0} = 1.5$  K. It is the only layered perovskite superconductor without Cu so far. Reduced  $T_c$ 's were achieved by using crystals containing impurities and defects. Moreover, in conjunction with the scaling relations (15) and (20) the experimental data on the  $T_c$  dependence of the in-plane correlation length, as well as the dependence of  $T_c$  on residual in plane resistivity, point to a 2D-QSI transition with  $z=1$  and  $\bar{\nu} \approx 1$ .<sup>28</sup> Thus, in agreement with the scaling predictions (22) and (27) for  $\beta_{T_c}$  versus  $T_{cm}/T_c$ ,  $\beta_{T_c}$  increases with reduced  $T_c$  and, as indicated by the solid curves in Fig. 5, tends to diverge as

$$\beta_{T_c} \approx 0.17 \frac{T_{cm}}{T_c}. \quad (28)$$

Note that the copper isotope effect in  $YBa_2Cu_3O_{7-\delta}$  (Ref. 29) leads to analogous behavior. Thus there is the remarkable experimental fact that  $\beta_{y_c}$ ,  $\beta_{p_u}$ , and  $\beta_{d_s}$  describing the shift of the critical point along the disorder, Cu substitution, dopant, and sheet resistance axis, respectively [see Eqs. (22) and (27)] adopt the nearly unique value  $\beta_{x_u} \approx \beta_{y_c} \approx \beta_{d_s} \approx 0.17-0.24$ , including the spin-triplet  $p$ -wave superconductor  $Sr_2RuO_4$ . It stems from a mechanism which shifts  $x_u$ ,  $y_c$  and  $d_s$  upon isotope substitution, subject to the intriguing constraint that the associated coefficient  $\beta_{x_u}$ ,  $\beta_{y_c}$ , and  $\beta_{d_s}$  adopt nearly the same value. As a consequence, in these ma-

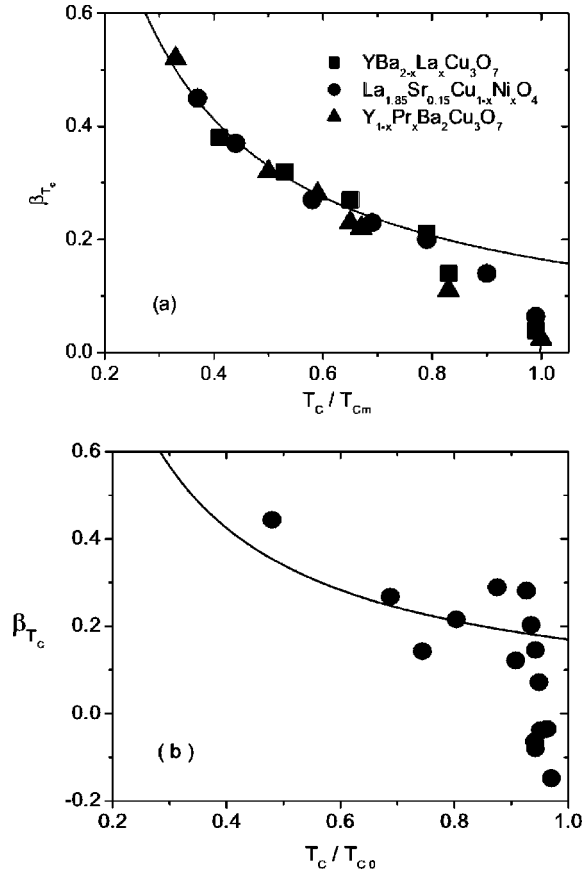


FIG. 5. (a)  $\beta_{T_c}$  versus  $T_c/T_{cm}$   $\text{YBa}_{2-y}\text{La}_y\text{Cu}_3\text{O}_7$  (Ref. 25),  $\text{La}_{1.95}\text{Sr}_{0.15}\text{Cu}_{1-y}\text{Ni}_y\text{O}_4$  (Ref. 26), and  $\text{Y}_{1-x}\text{Pr}_x\text{Ba}_2\text{Cu}_3\text{O}_7$  (Ref. 27). The solid curve is Eq. (28). (b)  $\beta_{T_c}$  versus  $T_c/T_{c0}$  for  $\text{Sr}_2\text{RuO}_4$ . Experimental data taken from Mao *et al.* (Ref. 16). The solid curve is Eq. (28).

materials the isotope effects and the pairing mechanism are unrelated. In this context it is important to note that the simultaneous occurrence of pairing and pair condensation requires the absence of thermal and quantum fluctuations. On the contrary, we have seen that cuprates flow, tuned by the combined effect of quantum fluctuations and disorder, to 2D-QSI criticality and that the isotope effects on transition temperature, specific heat, and penetration depths are not independent but related by the universal relation (11) which requires thermal fluctuations to dominate. Given this behavior it follows that along the flow to 2D-XY-QSI criticality fluctuations are relevant so that pairing and pair condensation do not occur simultaneously. The generically small value of  $\beta_{T_c}$  around the maximum transition temperature is then due to the cancellation of the specific heat and penetration depths contributions [Eq. (11)], while the rise of  $\beta_{T_c}$  with reduced  $T_c$  (Fig. 4) reflects the flow to 2D-XY-QSI criticality, where the scaling predictions (22), (27), and (28) apply.

We have seen that close to 2D-QSI criticality the isotope effects stem from the shift of the phase diagram and  $d_s$  upon isotope substitution. On the other hand, the 2D-QSI transition is driven by the exchange of pairs which favors superconductivity and the combined effects of disorder and Coulomb repulsion of the pairs, which favor localization. Since

isotope substitution will hardly affect disorder and Coulomb repulsion, the mechanism left is the electron-phonon interaction, which renormalizes the mass of the fermions and with that mass and exchange of the pairs. Indeed, inelastic neutron-scattering experiments on cuprate superconductors give clear evidence of a strong electron-phonon coupling.<sup>30</sup> In particular, characteristic phonon anomalies generated by a large electron-lattice interaction have been detected in  $\text{La}_2\text{CuO}_4$ .<sup>31-34</sup> Here a strong softening of the high-frequency copper-in-plane-oxygen bond-stretching modes is found as holes are doped in the insulating parent compound, i.e., we have an unmistakable and important example for a direct correlation of hole doping with the phonon anomalies. Doping leads to a strong decrease of the planar oxygen breathing mode frequency and even more strongly for a CuO bond-stretching vibration. Similar to the observations in doped  $\text{La}_2\text{CuO}_4$  pronounced phonon anomalies for the Cu-in-plane-oxygen bond stretching vibrations have also been observed by neutron scattering experiments in  $\text{YBa}_2\text{Cu}_3\text{O}_7$ .<sup>31,34</sup> These experimental results strongly suggest that the anomalous phonon softening upon hole doping and the associated strong electron-phonon coupling is a generic feature of cuprates. Moreover the measured frequency shift of the transverse optic phonons due to the substitution of  $^{16}\text{O}$  by  $^{18}\text{O}$  yielded in underdoped  $\text{YBa}_2\text{Cu}_3\text{O}_7$  ( $T_c=68$  K) an isotope coefficient of the expected magnitude for copper-oxygen stretching modes, with  $\beta_\omega=0.5\pm 0.1$ .<sup>35</sup>

#### IV. SUMMARY AND CONCLUSIONS

We have seen that the experimental data on the isotope effects on transition temperature and in-plane penetration depth in cuprate superconductors reveal remarkable consistency with the universal relations for a system undergoing a 3D-XY phase transition at finite temperature and a quantum superconductor to insulator transitions in two dimensions (2D-QSI). Although the relevant experimental data on the effect on transition temperature and in-plane penetration depth are rather sparse and the effect on the out-of-plane penetration depth and specific heat remains to be investigated, there is mounting evidence that cuprates fall at finite temperature into the 3D-XY and at zero temperature, close to the insulator-superconductor boundary into the 2D-XY-QSI universality classes. By definition, the universal relations hold irrespective of the dopant or substituent concentration. They apply whenever critical fluctuations dominate. In this case pairing and pair condensation do not occur simultaneously. This differs from conventional superconductors where fluctuations do not play an essential role and mean-field treatments appear to work. Here pairing and pair condensation occurs simultaneously and due to the absence of fluctuations the universal relations do not apply. Given then the analysis presented here, together with additional evidence for the importance of critical fluctuations in the cuprates, it becomes clear that the isotope effects in these materials do not provide direct information on the pairing mechanism. These effects are subject to the universal relations and the phase diagram. In the underdoped cuprates considered here, they provide useful information on the flow to

2D-QSI criticality and the interplay between the isotope effects on transition temperature, specific heat, and penetration depths. Concerning the mechanism of the isotope effects, it leads to a shift of the phase diagram.  $T_c$  is lowered and this implies unalterably a shift of the critical dopant, substituent, impurity, and defect concentration, where the 2D-QSI transition occurs. This transition is driven by the exchange of pairs, which favors superconductivity and the combined effects of disorder and Coulomb repulsion of the pairs, which favor localization. Since isotope substitution will hardly affect disorder and Coulomb repulsion, it appears most likely that electron-phonon interaction, which renormalizes the

mass of the fermions and with that the mass and the exchange of the pairs, is the relevant mechanism, giving rise to the shift of the phase diagram.

Finally we hope that this novel point of view about the isotope effects in fluctuation dominated superconductors will stimulate further experimental work to obtain new data to confirm or refute our predictions.

#### ACKNOWLEDGMENTS

The author is grateful to D. Di Castro, R. Khasanov, H. Keller, K. A. Müller, and J. Roos for stimulating discussions.

- 
- <sup>1</sup>J. Bardeen, Phys. Rev. **79**, 167 (1950).  
<sup>2</sup>G. Gladstone, M. A. Jensen, and J. R. Schrieffer, in *Superconductivity*, edited by R. D. Parks (Marcel Dekker, Inc., New York, 1969), p. 767.  
<sup>3</sup>J. R. Franck, in *Physical Properties of High Temperature Superconductors IV*, edited by D. M. Ginsberg (World Scientific, Singapore, 1994), p. 189.  
<sup>4</sup>T. Schneider and H. Keller, Int. J. Mod. Phys. B **8**, 487 (1993).  
<sup>5</sup>T. Schneider and H. Keller, Phys. Rev. Lett. **86**, 4899 (2001).  
<sup>6</sup>G. M. Zhao, M. B. Hunt, H. Keller, and K. A. Müller, Nature (London) **385**, 236 (1997).  
<sup>7</sup>G. M. Zhao, K. Conder, H. Keller, and K. A. Müller, J. Phys.: Condens. Matter **10**, 9055 (1998).  
<sup>8</sup>J. Hofer, K. Conder, T. Sasagawa, Guo-meng Zhao, M. Willemin, H. Keller, and K. Kishio, Phys. Rev. Lett. **84**, 4192 (2000).  
<sup>9</sup>R. Khasanov *et al.*, J. Phys.: Condens. Matter **15**, L17 (2003).  
<sup>10</sup>N. Momono, M. Ido, T. Nakano, M. Oda, Y. Okajima, and K. Yamaya, Physica C **233**, 395 (1994).  
<sup>11</sup>Y. Fukuzumi, K. Mizuhashi, K. Takenaka, and S. Uchida, Phys. Rev. Lett. **76**, 684 (1996).  
<sup>12</sup>T. Schneider, Europhys. Lett. **60**, 141 (2002).  
<sup>13</sup>T. Schneider, Physica B **326**, 289 (2003).  
<sup>14</sup>T. Schneider and J. M. Singer, *Phase Transition Approach To High Temperature Superconductivity* (Imperial College Press, London, 2000).  
<sup>15</sup>T. Schneider, cond-mat/0204236 (unpublished).  
<sup>16</sup>Z. Q. Mao, Y. Maeno, Y. Mori, S. Nimori, and M. Udagawa, Phys. Rev. B **63**, 144514 (2001).  
<sup>17</sup>M. P. A. Fisher, G. Grinstein, and S. M. Girvin, Phys. Rev. Lett. **64**, 587 (1990).  
<sup>18</sup>M. C. Cha, M. C. Cha, M. P. A. Fisher, S. M. Girvin, M. Wallin, and P. A. Young, Phys. Rev. B **44**, 6883 (1991).  
<sup>19</sup>I. F. Herbut, Phys. Rev. B **61**, 14 723 (2000).  
<sup>20</sup>P. C. Hohenberg, A. Aharony, B. I. Halperin, and E. P. Siggia, Phys. Rev. B **13**, 2986 (1976).  
<sup>21</sup>See, e.g., M. Ma, *Modern Theory of Critical Phenomena* (Benjamin, Reading, MA, 1976).  
<sup>22</sup>M. R. Presland *et al.*, Physica C **176**, 95 (1991).  
<sup>23</sup>J. L. Tallon, C. Bernhard, H. Shaked, R. L. Hitterman, and J. D. Jorgensen, Phys. Rev. B **51**, 12 911 (1995).  
<sup>24</sup>A. G. Sun, L. M. Paulius, D. A. Gajewski, M. B. Maple, and R. C. Dynes, Phys. Rev. B **50**, 3266 (1994).  
<sup>25</sup>H. J. Bornemann and D. E. Morris, Phys. Rev. B **44**, 5322 (1991).  
<sup>26</sup>N. Babushkina *et al.*, Physica C **185–189**, 901 (1991).  
<sup>27</sup>J. P. Franck *et al.*, Phys. Rev. B **44**, 5318 (1991).  
<sup>28</sup>Z. Q. Mao, Y. Mori, and Y. Maeno, Phys. Rev. B **60**, 610 (1999).  
<sup>29</sup>Guo-Meng Zhao *et al.*, Phys. Rev. B **54**, 14 956 (1996).  
<sup>30</sup>L. Pintschovius and W. Reichardt, in *Neutron Scattering in Layered Copper-Oxide Superconductors*, edited by A. Furrer, Physics and Chemistry of Materials with Low Dimensional Structures Vol. 20 (Kluwer Academic, Dordrecht, 1998), p. 165.  
<sup>31</sup>L. Pintschovius and M. Braden, J. Low Temp. Phys. **105**, 813 (1996).  
<sup>32</sup>R. J. McQueeney, Y. Petrov, T. Egami, M. Yethiray, G. Shirane, and Y. Endoh, Rev. Plasma Phys. **82**, 628 (1999).  
<sup>33</sup>L. Pintschovius and M. Braden, Phys. Rev. B **60**, R15 039 (1999).  
<sup>34</sup>W. Reichardt, J. Low Temp. Phys. **105**, 807 (1996).  
<sup>35</sup>N. L. Wang *et al.*, Phys. Rev. Lett. **89**, 087003 (2002).